Mode decomposition of Kerr self-cleaned beams by phase only SLM

Denis S. Kharenko[a,b], Mikhail D. Gervaziev[a,b], Innokentiy Zhdanov[a,b], Evgeniy V. Podivilov[a,b], Sergey A. Babin[a,b], and Stefan Wabnitz[a,c]

[a]Novosibirsk State University, 1 Pirogova str., Novosibirsk, Russian
[b]Institute of Automation and Electrometry SB RAS, 1 Ac. Koptyug ave., Novosibirsk, Russian
[c]DIET, Sapienza University of Rome, Via Eudossiana 18, 00184 Rome, Italy

ABSTRACT

Graded-index multimode optical fibers have recently attracted a renewed attention, thanks to the discovery of new nonlinear effects, such as Kerr beam self-cleaning. In essence, Kerr self-cleaning involves a flow of the propagating beam energy into the fundamental mode of the fiber, accompanied by a redistribution of the remaining energy among high-order modes. Increasing the fundamental mode energy leads to a significant improvement of the output beam quality. A standard method to determine beam quality is to measure the M^2 parameter. However, since self-cleaning involves the nonlinear redistribution of energy among a large number of fiber modes, measuring a single beam quality parameter is not sufficient to characterize the effect. A properly informative approach requires performing the mode decomposition of the output beam. Mode decomposition permits to evaluate the energy distribution among all of the excited fiber modes, which enables investigations of nonlinear mode coupling processes at a qualitatively new level. In this work, we demonstrate an efficiency mode decomposition method based on holography, which is suitable for analyzing the self-cleaning effect. In a theoretical study, we describe the solution of the mode decomposition problem for the modes of the graded-index multimode fiber. In an experimental investigation, we demonstrate the decomposition of both low-power (speckled) and self-cleaned beams, involving more than 80 modes.

Keywords: beam characterization, spatial light modulation, mode decomposition, GRIN multi-mode fibers

1. INTRODUCTION

Interest in optical multimode fibers (MMF) has experienced different periods of rise and fall, but today we are witnessing a rapid increase of research activity involving MMFs. The main problem with the practical use of MMFs is the relatively low quality of laser beams at their output, when compared with single mode fibers (SMFs). The output beam quality severely decreases, as the number of the excited modes grows larger.[1,2] However, in recent years there has been a resurgence of research interest in MMFs, and several novel nonlinear effects have been observed. Among them, perhaps the most intriguing phenomenon involves the observation of a nonlinear redistribution of the input beam energy among the modes of a GRIN MMF. Nonlinear mode coupling leads to the formation of a stable, bell-shaped beam profile at the MMF output, accompanied by a significant improvement of the beam quality: this effect has been called Kerr beam self-cleaning.[3] When considering nonlinear processes leading to changes in the mode distribution, modal decomposition (MD) is the natural technique for their quantitative and qualitative experimental characterization. There are several approaches to perform MD, based on different methods and algorithms. Conceptually, these methods can be divided into several groups, depending on the foundation lying beneath them: genetic algorithms,[4] adaptive optics,[5] digital holography with spatial light modulators (SLM),[6] mode-cross correlation analysis (C^2),[7] beam characterization in terms of spatiotemporal (TERMITES)[8] or spatial-spectral (S^2)[9] distributions. It is important to mention that some MD techniques can be used sequentially, in order to make the whole MD procedure faster. For example, a genetic algorithm can be applied for the evaluation of the modal phases, which are associated with the set of

Further author information: (Send correspondence to D.S.Kh.)
D.S.Kh.: E-mail: kharenko@iae.nsk.su

intensities that are initially extracted out of experimental measurements. In addition, multiple amplitudes can be measured in parallel from one shot.[10]

In this work, we propose and apply the MD with phase-only SLM digital holography generation to the study of the Kerr beam self-cleaning effect.[11] The impact of the phase-mask size, and of the true meaning point search procedure are among the several crucial factors that affect the accuracy of the MD procedure, and they will be discussed in details in our presentation. This permits us to successfully demonstrate the application of our MD method to characterize the effect of beam self-cleaning, by studying the evolution of the output distribution of mode energies as the input power grows larger. Specifically, we show that an asymptotic stable mode distribution dominated by the fundamental mode of the fiber is stably reached at high powers, in good qualitative agreement with theoretical predictions. An additional important result of our studies is the first, to our knowledge, demonstration of the modal polarization dynamics of beam self-cleaning, which permits to shed a new light on the self-cleaning polarization dynamics, that was initially studied in Ref.[12]

2. MODE DECOMPOSITION EXPERIMENT

Although different aspects of the MD procedure have been described in the literature,[11,13–15] its practical implementation still remains a rather challenging task. This is because of the presence of some hidden key parameters, such as the picket-fence effect, which are extremely important for obtaining correct results, that is, for successfully reconstructing a multimode laser beam based on the MD results. In this section we will describe two of the main issues that unavoidably arise when performing MD measurements.

2.1 Experimental setup

The experimental MD scheme is presented in Fig. 1. The fiber under test is a 3 m long span of standard GRIN MMF, with 50 µm core diameter. The fundamental mode radius of the fiber w_0 is equal to 6.33 µm, and the measured input beam radius is 15 µm (at the $1/e^2$ level of peak intensity). Lenses 1 and 2 were used to magnify the output beam size at the SLM display by about 150 times, in order to increase the effective resolution. Our SLM operates in the horizontal polarization: therefore, we use a polarization beam splitting (PBS) cube and an half-wave plate in front of it, in order to switch the output polarization state. In our experiments, the size of the phase-mask encoded by the SLM must be suffiicently close to the size of the beam at the display, in order for the measured mode amplitudes to correspond to the actual fiber modes. It is important to note that by the size of the phase-mask we mean the radius of the fundamental mode (at the $1/e$ level of the field), for which it was calculated. The measurements should be taken at the point of interest (POI), which corresponds to the center of the first diffraction maximum: this point is marked as (q, q) in Fig. 1. The algorithms which permit to estimate both of these parameters will be explained in the following sub-sections.

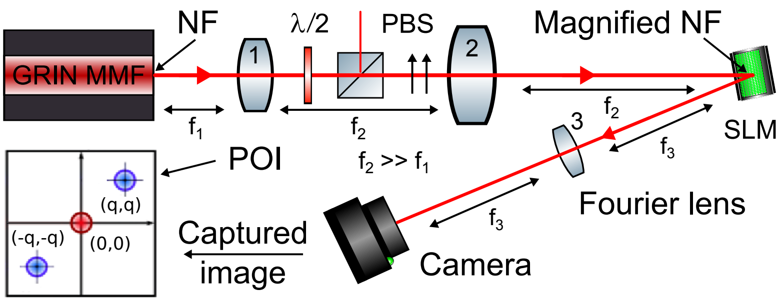

Figure 1. Mode decomposition experimental setup.

2.2 Point of Interest

The main property, upon which MD is based, is that the Fourier transform of the field captured at the proper point, is equal to computing a dot product. As a result, the beam intensity in the Fourier plane is proportional to the square modulus of the mode amplitude. The point of capture can be moved across the transverse plane

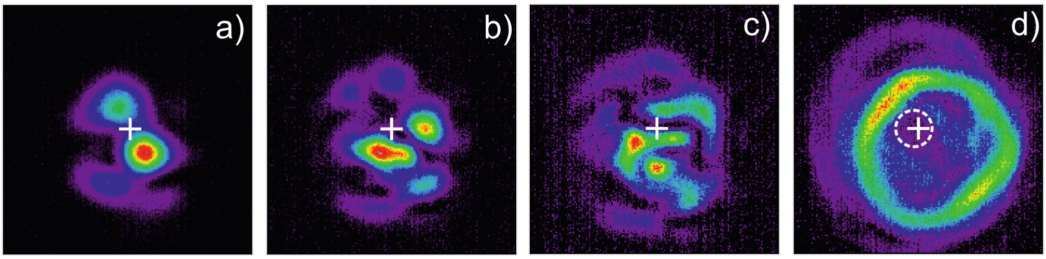

Figure 2. Measured correlation functions at the first-order diffraction maximum for the LG_{00} mode (a), LG_{01} mode (b), LG_{02} mode (c), and sum of the pictures for higher-order modes (with the highest principal mode number n) (d).

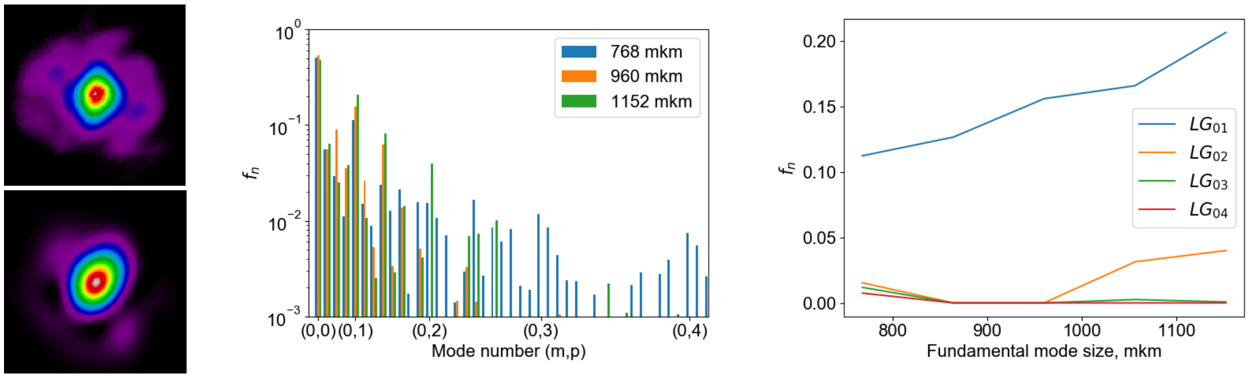

a) b) c)

Figure 3. a) Measured (top) and reconstructed beams; b) Mode energy distribution vs. mode number (defined through the azimuthal index m and radial index p), for different sizes of the phase mask; c) Contribution of high-order radial modes as a function of the size of the phase mask.

by introducing a spatial frequency shift into a phase mask, which is used to overcome the limitation of phase-only SLMs, thus encoding both phase and amplitude of a selected mode,[16] or for the parallel measurement of several modes.[10,13] However, the problem is that the position of the capturing point is hard to determine in an experiment, especially in the case of speckled beams. The difficulty is worsened by the high sensitivity of the decomposition results with respect to any positioning error. It was shown numerically[11] that a mismatch of a few pixel only can lead to more than 10% relative error in the mode amplitudes, which results in significant visual differences between original and reconstructed beams. In that same paper, we proposed an experimental method that can solve this problem. The method involves looking at the first diffraction maximum, where the required intensity value is located. Examples of captured images of the first diffraction maximum for different low-order modes are shown on Fig. 2(a)–(c). In our method, we assume that the point of interest (POI) is the same for all of the captured images, and that high-order modes only contain a relatively small portion of the beam energy, so that the POI has a minimal intensity for all of them. In Fig. 2(d) we report such integrated images for several of the higher-order modes with the largest main quantum number. Since the intensity distribution of the first diffraction maximum in the remaining area is random, and the required POI has the lowest level of intensity, the point of local minimum near the center of the averaged picture can be clearly visualized (it is circled by a dotted line in Fig. 2(d)). This permits to perform several beam reconstructions (a few dozens is enough) by iterating over the points from this limited area, eventually obtaining the most suitable result.

2.3 Size of the phase-mask

An important task in the preparation of the experiment, is the choice of the optimal size of the phase mask. In order to define this parameter, one needs to find out the beam size on the SLM. We used the ABCD matrix algorithm, in order to describe beam propagation in the optical setup from the fiber output up to the SLM. Numerical simulation made earlier, demonstrated that a mismatch of the phase mask size leads to an increase of errors in the amplitude and phase retrieval. These errors increase proportionally to the mask size deviation from its optimum value.

In order to find out the optimal size of the phase mask, we have done several MD iterations for the same beam in the self-cleaned regime, when the beam energy remains concentrated in the fundamental mode and a few low-order modes only. In this case, we may assume that the contribution of higher-order radial modes tends to zero when the size of magnified fundamental mode of the fiber and the size used in the calculation of the phase mask become equal. Phase mask sizes in the range from 768 µm to 1152 µm were chosen. The reconstruction results are shown on Fig. 3.a, and they all reproduce the measured beam very well. To see the difference, we plot mode distributions in a logarithmic scale (see Fig. 3.b). As it can be clearly seen, the amount of excited modes is much larger for a radius of 768 µm. To find the optimum value of the phase mask size, we only take radial modes, and plot their energy as a function of the mask size (see Fig. 3.c). As can be seen, a minimum around 900 µm is obtained. Detailed measurements show that the optimal value is found at 936 µm, a value that we shall use in all of our subsequent experiments.

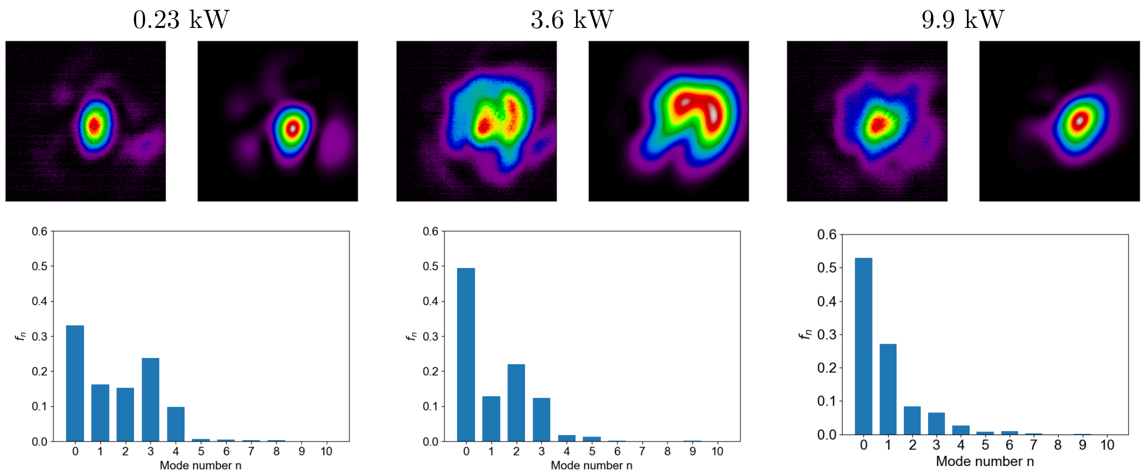

Figure 4. Input peak power dependence of the measured intensity distribution (left in the top blocks) and retrieved through the MD procedure (right in the top blocks), together with the relative energy distribution (bottom), averaged over degenerate modes.

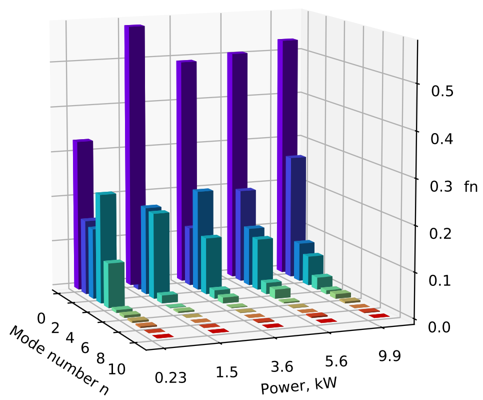

Figure 5. Retrieved energy distributions as a function of input peak power. Colors correspond to different mode numbers.

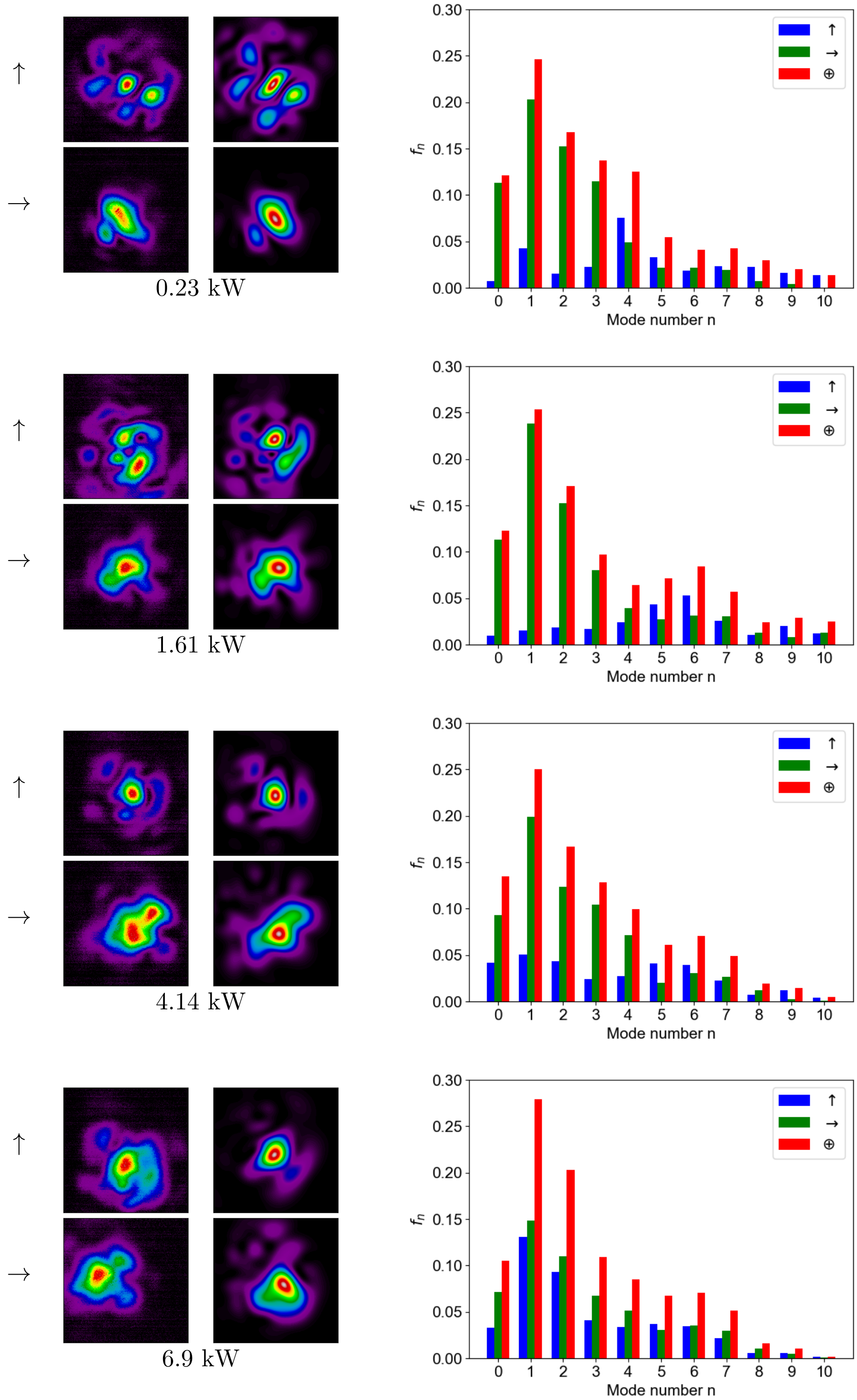

Figure 6. Retrieved energy distributions vs. input peak power, evaluated for both orthogonal polarization components, which are denoted as ↑ and →. Histograms on the right-hand side contain three bins for each mode number, where the first and the second bin correspond to orthogonal polarizations, and the third corresponds to their sum (⊕), i.e., the total energy in a given mode number.

3. RESULTS AND DISCUSSION

3.1 Mode dynamics for self-cleaned beams

As discussed in the previous section, the key hidden parameters in the MD procedure have been identified and optimized. Therefore, in this section we may apply our non-iterative MD method to the study of the nonlinear dynamics of the power-dependent re-distribution of energy among the modes that carry laser beams in GRIN fibers. In addition, we also take into account the mode evolution across both polarization components of the beam.

The first series of experiments involved beams emerging with a small degree of ellipticity from the GRIN fiber output. In this case, we adjusted the wave-plate in order to obtain a maximum of power after the PBS (see Fig. 1), and we performed the MD for different input peak powers. The corresponding results are depicted in Fig. 4, where the top intensity distributions are presented for a qualitative verification of the MD accuracy (by comparing measured and reconstructed beams), and bottom histograms illustrate the relative energy distribution, averaged over degenerate modes. This averaging is based on the assumption that coupling for modes with an equal mode number is much higher than for modes from different groups. Such mode coupling is induced by various fiber imperfections. Whereas coupling between modes with different mode number is only provided by nonlinear interactions. This behavior was also confirmed by theoretical models.[17] Besides, a smaller number of integral parameters makes the the MD results much easier to analyze. We denote such parameters as f_n, according to our previous work.[18] As one can see, the mode energy distribution changes from a random initial state, and it approaches an equilibrium distribution as the input power grows larger. Fig. 5 shows the power evolution of the output mode distribution step-by-step: as can be seen, the last two histograms do not differ that much, which confirms that a stable mode distribution is reached at high powers.

The second series of experiments involved the MD of both polarization components of the output beam. We switched between polarizations by rotating the half wave-plate (Fig. 1), so that each power level was decomposed twice. The relative power was extracted, in order to normalize the retrieved mode amplitudes. Our results also show that, in this case, the output beam has a significant degree of ellipticity. The corresponding results are depicted in Fig. 6. Here the left column with the blocks of four patterns corresponds to the measured beam intensity profiles (left column in blocks), along with the corresponding retrieved beam intensities (right column in blocks). Different polarizations are denoted as $\uparrow$ (top row in blocks) and $\rightarrow$ (bottom row in blocks). The histograms showing the corresponding mode energy distributions are presented on the right column of Fig. 6.

As one can see, retrieved and measured intensity profiles are very close to each other, for all cases. This permits us to conclude that the MD method is accurate enough. What is more interesting is that the effect of Kerr beam self-cleaning into the fundamental mode of the fiber does not manifest here, in contrast with the case of Figs. 4- 5. In fact, in spite of the significant changes in the intensity profiles, we observe no significant nonlinear interactions, leading to a flow of energy into the fundamental mode of the fiber. Relative energy distributions for both orthogonal states of polarization (red bins) only show little changes from the initial state.

In order to explain this behavior, we may notice that, in contrast with the case of Figs. 4- 5, where the fundamental mode with $n = 0$ is already initially most populated, in Fig. 6 the input mode distribution leads to a dominant presence of the $n = 1$ mode: in this case, it was previously observed that self-cleaning in the fundamental mode can be prevented, to the advantage of the higher-order mode.[19]

Additionally, it is interesting to compare the energy evolution between polarizations inside a given mode number (blue and green bins). As it can be clearly seen, for the last three peak power values (1.61, 4.14 and 6.9 kW) the relative power changes monotonically for $n = 1, 2, 3$. This amounts to the effect of nonlinear polarization rotation in a GRIN fiber, as reported in recent experiments.[12] As a result, each mode experiences a different rotation of its state of polarization with power, which may reduce nonlinear mode coupling, hence power transfer among non-degenerate modes.

4. CONCLUSION

In this work, we have investigated the nonlinear dynamics of Kerr self-cleaned beams by using the method of mode decomposition. Hidden parameters of the experimental setup, such as the best measurement point (point of interest) and the size of the phase mask, have been discussed. Our MD method allows for obtaining the mode energy distribution even in the case of a relatively large number of modes (∼80) in each polarization. Two distinct mode dynamics were observed. In the first case, when the $n = 0$ mode is already initially dominant, the energy distribution tends to an equilibrium state, with a significant flow of energy towards the fundamental mode of the fiber. In the second case, where the $n = 1$ mode has the highest energy at the fiber input, the effect of nonlinear polarization evolution is observed, with only minor nonlinear power transfers among the modes. In conclusion, use of the MD method is essential for studying power-induced beam reshaping in MMFs, as it permits to disclose the dependence of the nonlinear mode distribution as a function of the input beam conditions.

ACKNOWLEDGMENTS

This work was supported by the Russian Ministry of Science and Education (Grant No. 14.Y26.31.0017). M.G. was also supported by RFBR (Grant No. 20-32-90132), S.B. and D.Kh were supported by RSF (Grant No. 21-42-00019). S.W. was also supported by the European Research Council (Grant. No. 740355 and No. 874596).

REFERENCES

[1] Paschotta, R., "Single-mode fibers." RP Photonics Encyclopedia https://www.rp-photonics.com/single_mode_fibers.html. (Accessed: 11 February 2021).

[2] Li, Z., Zhou, J., He, B., Lou, Q., and Xue, D., "Beam quality of multimode fiber lasers using coiling technique," *Optik-International Journal for Light and Electron Optics* **124**(1), 82–84 (2013).

[3] Krupa, K., Tonello, A., Shalaby, B. M., Fabert, M., Barthelemy, A., Millot, G., Wabnitz, S., and Couderc, V., "Spatial beam self-cleaning in multimode fibres," *Nat. Photonics* **11**(4), 237–241 (2017).

[4] Li, L., Leng, J., Zhou, P., and Chen, J., "Multimode fiber modal decomposition based on hybrid genetic global optimization algorithm," *Optics Express* **25**(17), 19680 (2017).

[5] Schulze, C., Naidoo, D., Flamm, D., Schmidt, O. A., Forbes, A., and Duparré, M., "Wavefront reconstruction by modal decomposition," *Optics Express* **20**(18), 19714 (2012).

[6] Flamm, D., Naidoo, D., Schulze, C., Forbes, A., and Duparré, M., "Mode analysis with a spatial light modulator as a correlation filter," *Optics Letters* **37**(13), 2478 (2012).

[7] Schimpf, D. N., Barankov, R. A., and Ramachandran, S., "Cross-correlated (c2) imaging of fiber and waveguide modes," *Opt. Express* **19**(14), 13008–13019 (2011).

[8] Pariente, G., Gallet, V., Borot, A., Gobert, O., and Quéré, F., "Space–time characterization of ultra-intense femtosecond laser beams," *Nature Photonics* **10**(8), 547–553 (2016).

[9] Nicholson, J., Yablon, A. D., Ramachandran, S., and Ghalmi, S., "Spatially and spectrally resolved imaging of modal content in large-mode-area fibers," *Optics express* **16**(10), 7233–7243 (2008).

[10] Zhao, Y., Huang, S., and Yan, C., "Parallel measurement of multiple linear polarization modes in few-mode optical fibers using spatial light modulators," *Opt. Eng.* **58**(09), 1 (2019).

[11] Gervaziev, M. D., Zhdanov, I., Kharenko, D. S., Gonta, V. A., Volosi, V. M., Podivilov, E. V., Babin, S. A., and Wabnitz, S., "Mode decomposition of multimode optical fiber beams by phase-only spatial light modulator," *Laser Phys. Lett.* **18**(1), 015101 (2021).

[12] Krupa, K., Garmendia Castañeda, G., Tonello, A., Niang, A., Kharenko, D. S., Fabert, M., Couderc, V., Millot, G., Minoni, U., Modotto, D., and Wabnitz, S., "Nonlinear polarization dynamics of Kerr beam self-cleaning in a graded-index multimode optical fiber," *Opt. Lett.* **44**(1), 171 (2019).

[13] Kaiser, T., Flamm, D., Schröter, S., and Duparré, M., "Complete modal decomposition for optical fibers using CGH-based correlation filters," *Opt. Express* **17**(11), 9347 (2009).

[14] Flamm, D., Schulze, C., Naidoo, D., Schroter, S., Forbes, A., and Duparre, M., "All-digital holographic tool for mode excitation and analysis in optical fibers," *J. Light. Technol.* **31**(7), 1023–1032 (2013).

[15] Forbes, A., Dudley, A., and McLaren, M., "Creation and detection of optical modes with spatial light modulators," *Adv. Opt. Photonics* **8**(2), 200 (2016).

[16] Arrizón, V., Ruiz, U., Carrada, R., and González, L. A., "Pixelated phase computer holograms for the accurate encoding of scalar complex fields," *J. Opt. Soc. Am. A* **24**(11), 3500 (2007).

[17] Sidelnikov, O. S., Podivilov, E. V., Fedoruk, M. P., and Wabnitz, S., "Random mode coupling assists Kerr beam self-cleaning in a graded-index multimode optical fiber," *Opt. Fiber Technol.* **53**(September), 101994 (2019).

[18] Podivilov, E. V., Kharenko, D. S., Gonta, V. A., Krupa, K., Sidelnikov, O. S., Turitsyn, S., Fedoruk, M. P., Babin, S. A., and Wabnitz, S., "Hydrodynamic 2D Turbulence and Spatial Beam Condensation in Multimode Optical Fibers," *Phys. Rev. Lett.* **122**(10), 103902 (2019).

[19] Deliancourt, E., Fabert, M., Tonello, A., Krupa, K., Desfarges-Berthelemot, A., Kermene, V., Millot, G., Barthélémy, A., Wabnitz, S., and Couderc, V., "Kerr beam self-cleaning on the LP11 mode in graded-index multimode fibers," *OSA Continuum* **2**, 1089–1096 (Apr 2019).